Biochemical Pharmacology 77 (2009) 1437–1444

Contents lists available at ScienceDirect

Biochemical Pharmacology

journal homepage: www.elsevier.com/locate/biochempharm

Effects of the anthelmintic drug PF1022A on mammalian tissue and cells

R. Dornetshuber [a,b], M.R. Kamyar [a], P. Rawnduzi [a], I. Baburin [a], K. Kouri [a], E. Pilz [a], T. Hornbogen [c], R. Zocher [c], W. Berger [b], R. Lemmens-Gruber [a,*]

[a] Department of Pharmacology and Toxicology, University of Vienna, Althanstr. 14, A-1090 Vienna, Austria
[b] Institute of Cancer Research, Department of Medicine I, Borschkegasse 8a, Medical University of Vienna, 1090 Vienna, Austria
[c] Technical University of Berlin, Franklinstr. 29, D-10587 Berlin, Germany

ARTICLE INFO

Article history:
Received 28 November 2008
Accepted 8 January 2009

Keywords:
PF1022A
Anthelmintics
Ionophore
Cytotoxicity
Apoptosis

ABSTRACT

Nematode infections cause human morbidity and enormous economic loss in livestock. Since resistance against currently available anthelmintics is a worldwide problem, there is a continuous need for new compounds. The cyclooctadepsipeptide PF1022A is a novel anthelmintic that binds to the latrophilin-like transmembrane receptor important for pharyngeal pumping in nematodes. Furthermore, PF1022A binds to GABA receptors, which might contribute to the anthelmintic effect. Like other cyclodepsipeptides, PF1022A acts as an ionophore. However, no correlation between ionophoric activity and anthelmintic properties was found. This is the first study describing the effect of PF1022A on mammalian cells and tissues. While channel-forming activity was observed already at very low concentrations, changes in intracellular ion concentrations and reduction of contractility in isolated guinea pig ileum occurred at multiples of anthelmintically active concentrations. PF1022A did not induce necrotic cell death indicated by complete lack of cellular lactate dehydrogenase release. In contrast, apoptosis induction via the mitochondrial pathway was suggested for long-term drug treatment at high concentrations due to numerous apoptotic morphological changes as well as mitochondrial membrane depolarisation. Short time effects were based on cell cycle blockade in G_0/G_1 phase. Additionally, the cell cycle and apoptosis regulating proteins p53, p21 and bax, but not Bcl-2 were shown to impact on PF1022A-induced cytotoxicity. However, since PF1022A-induced cytotoxicity was found at drug concentrations higher than those used in anthelmintic treatment, it can be suggested that PF1022A intake might not impair human or animal health. Thus, PF1022A seems to be a safe alternative to other anthelmintic drugs.

1. Introduction

Nematode infections are a major cause of human morbidity and mortality in tropic and temperate climates [1]. Moreover, these pathogens cause enormous economic loss in cattle, horses, pigs and sheep [2,3]. However, resistance against the major currently available anthelmintics has increasingly become a worldwide problem [4]. Therefore, new compounds with different modes of action are needed to manage the problem of resistance. The 24-membered N-methylated cyclooctadepsipeptide PF1022A belongs to a novel class of anthelmintic agents with potent broadspectrum anthelmintic activity and low toxicity in animals [5–9]. Additionally this drug was found to be a good candidate for the treatment of human angiostrongyliasis [10].

PF1022A is a secondary metabolite of the fungus imperfectus *Mycelia sterilia* (*Rosellinia* sp.) isolated from the plant *Camellia japonica* [5]. So far, the nonribosomal N-methyl-cyclooctadepsipeptide synthetase responsible for PF1022A biosynthesis has been isolated and characterized [11]. Consequently, this discovery allows the development of new N-methyl-cyclooctadepsipeptide-derived compounds [12]. PF1022A serves as starting material for the synthesis of semi-synthetic cyclooctadepsipeptide derivatives with improved anthelmintic potency and broadspectrum activity [13–16]. Meanwhile, also total synthesis of cyclooctadepsipeptides has been accomplished [17–22].

With regard to the molecular mechanisms underlying its anthelmintic activity, PF1022A has been shown to bind to the amine terminus of the 110-kDa heptahelical, latrophilin-like transmembrane receptor HC-110R, isolated from *Haemonchus contortus* (Rudolphi). This receptor has an important regulatory function on pharyngeal pumping in nematodes. By binding to this receptor, PF1022A induces an influx of external Ca^{2+} into the cell [23], consequently affecting several presynaptic signal transduction pathways [24]. Due to this effect, treatment with PF1022A as well as the semi-synthetic emodepside causes worm paralysis [24,25]. These modes of action are different from the mechanisms

* Corresponding author. Tel.: +43 1 4277 55325; fax: +43 1 4277 9553.
E-mail address: rosa.lemmens@univie.ac.at (R. Lemmens-Gruber).

0006-2952/$ – see front matter © 2009 Elsevier Inc. All rights reserved.
doi:10.1016/j.bcp.2009.01.005

of known anthelmintics like benzimidazoles, imidazothiazoles, tetrahydropyrimidines and macrocyclic lactones [26]. Thus, these new drugs might solve the increasing problem of resistance development against available anthelmintics. Indeed, PF1022A and emodepside were effective in benzimidazole-, levamisol- and ivermectin-resistant populations of *H. contortus* in sheep when applied orally, subcutaneously or intravenously. Additionally, they showed activity in ivermectin-resistant *Cooperia oncomorpha* population in cattle [3]. Furthermore, in binding studies it could be demonstrated that PF1022A binds to GABA receptors in nematodes, which might contribute to the anthelmintic effect [27]. PF1022A acts as an ionophore in planar lipid bilayers like other cyclodepsipeptides, however, testing structurally related derivates revealed no correlation between ionophoric activity and anthelmintic properties [28].

However, at least to our knowledge, no data describing the effect of PF1022A on mammalian cells and tissues are published so far. PF1022A is structurally related to cyclohexadepsipeptides of the enniatin-type for which synergistic effects on antifungal drug activity were described [29,30]. Moreover, potent cytostatic and cytotoxic effects against diverse cancer cell types [31–33], antiangiogenic activity [34] as well as anthelmintic properties [35] could be demonstrated for these structurally related cyclohexadepsipeptides.

Aim of this study was to investigate the effect of PF1022A on force of contraction in isolated guinea pig ileum, its electrophysiological properties and the resulting impacts on cell homeostasis. Moreover, PF1022A-induced cytotoxic modes of action were elucidated in mammalian cells.

2. Materials and methods

2.1. Test compound

PF1022A was kindly supplied by Bayer AG, Germany. The compound is poorly soluble in water, therefore a stock solution with Tween 80:MeOH = 1:2 (Sigma–Aldrich, Vienna, Austria) was prepared. This solution was further diluted to the nutrient solution at the final concentration.

2.2. Cell lines

The following human cell lines were used in this study: the epidermal carcinoma-derived cell line KB-3-1 (generously donated by Dr. Shen, Bethesda, USA) [36], the colon carcinoma cell line CaCo-2 (American Tissue Culture Collection), the colon carcinoma cell model HCT116 and respective sublines with deleted p53, p21, or bax genes (generously donated by Dr. Vogelstein, John Hopkins University, Baltimore) [37–39], the Bcl-2-negative non-small cell lung cancer cell line A549 and its bcl-2 pBabe/Puro-transfected subline [31]. HCT116 cell lines were grown in McCoy's culture medium, Caco-2 cells in MEME, and KB-3-1 as well as A549 cells and the transfected subline in RPMI 1640 medium. All culture media were purchased from Sigma–Aldrich GmbH (St. Louis, MO) and supplemented with 10% fetal calf serum (PAA, Linz, Austria). Cultures were periodically checked for *Mycoplasma* contamination.

2.3. Contractility measurement

The effect of PF1022A on force of contraction (f_c) of isolated terminal ilea of the guinea pig was studied as previously described [40]. All chemicals were purchased by Sigma–Aldrich (Vienna, Austria). The test compound was added cumulatively to the bathing solution in rising concentrations every 30 min when a steady-state effect has been reached.

2.4. Ionophoric activity—single channel current

Electrical activity was studied on CaCo-2 cells at room temperature (19–22 °C) as previously described [40,48]. Chemicals for pipette and bathing solutions were supplied by Sigma–Aldrich (Vienna, Austria). After a control period of 15 min during which no electrical activity could be observed, PF1022A was added to the bathing solution. The wash-in phase lasted about 1–2 min until single channel current could be detected. The same experimental protocol (E_h = −60, −40, −20, 0, +20, +40, +60 mV) was applied as during control recordings.

Electrophysiological measurements were carried out with an Axopatch-1D patch clamp amplifier (Axon Instruments, CA) at a cut-off frequency (−3 dB) of 2 kHz. Currents were filtered at 5 kHz with a dual variable filter (VBF 8, Kemo Ltd, Beckenham, Kent, UK), digitized via an AD converter (TL-1 interface, Axon Instruments, CA) and sampled at 5–10 kHz. Data acquisition and storage were processed directly to a PC equipped with pCLAMP 6 software (Axon Instruments, CA). Single channel analysis was performed with the ASCD software (G. Droogmans, Leuven, Belgium).

2.5. Two-microelectrode voltage clamp studies—$GABA_A$ receptor

Stage V–VI oocytes from *Xenopus laevis* were prepared and cRNA injected as previously described [41,42]. On the 2nd day after cRNA injection, electrophysiological experiments were performed by the two-microelectrode voltage clamp method using of a TURBO TEC 01C amplifier (npi electronic GmbH, Tamm, Germany) at a holding potential of −70 mV. The bath solution contained 90 mM NaCl, 1 mM KCl, 1 mM $MgCl_2$, 1 mM $CaCl_2$ and 5 mM HEPES (pH 7.4). PF1022A was co-applied with GABA $EC_{3\text{-}10}$ (effective concentration of GABA that induces 3–10% of maximal GABA-evoked current) by means of an automated fast perfusion system according to [43]. Percent potentiation of I_{GABA} by the PF1022A was calculated using formula: $(R/C) \times 100\%$, where R is the amplitude of the chloride current evoked by co-application of control GABA $EC_{3\text{-}10}$ and the indicated concentration of the compound, and C is the amplitude of the chloride current evoked by application of control GABA $EC_{3\text{-}10}$ alone.

2.6. Fluorescence imaging

Caco-2 cells were loaded with 1 μM FURA 2AM and an equivalent concentration of Pluronic 20% in DMSO at room temperature (18–23 °C) for 30–45 min. Fluorescent dye and Pluronic were procured from Molecular Probes (Leiden, The Netherlands). After washout cells were allowed to hydrolyze the dye for 30 min to 1 h, and experiments were performed as previously described [47]. Ratiometric measurements were realized following background subtraction with the Axon Imaging Workbench 2.2 software (Axon Instruments, CA) averaging 2 frames. Results are presented as the relative change ($-\Delta F/F_o$) of the F_{340}/F_{380} signal.

2.7. Cell viability assays

KB-3-1 cells were seeded (2×10^4 cells/ml) in 96-well plates and were allowed to recover for 24 h. Concentrations of PF1022A ranging from 0.5 up to 10 μM were applied with an incubation time of 24, 48 and 72 h. The cytotoxic effect of PF1022A was determined with an MTT-based vitality assay (EZ4U, Biomedica, Vienna, Austria) as described previously [31]. Moreover, to study the reversibility of the cytotoxic PF1022A effect, after an incubation time of 1, 2, 4, 6, 8, 24 and 48 h the test compound was removed from the wells and substituted by fresh medium. After a total incubation period of 72 h the EZ4U assay was

performed and data were evaluated using the GraphPadPrism 4 software.

2.8. Lactate dehydrogenase release assay

The release of lactate dehydrogenase (LDH) from the cytosol, which indicates loss of membrane integrity and is further associated with necrotic cell death, was studied with a cytotoxicity detection kit (Roche, Basel, Switzerland). Adherent KB-3-1 cells (2×10^4 cells/ml) were incubated in 96-well plates for 24 h with PF1022A (0.5–10 μM). Afterwards, from each well 100 μl of the supernatant was transferred to a 96-well microplate and incubated for 20 min at 37 °C with reagent solution of the kit according to the manuel. Finally, absorbance was measured with a microplate reader, set at 490 and 620 nm as reference.

2.9. DAPI staining

1×10^5 KB-3-1 cells/well were treated in 6 well plates with 2.5–10 μM PF1022A for 24 and 48 h, respectively. Subsequently, cells were harvested, cytospins were prepared, and apoptosis was evaluated by staining with 4′,6-diamidino-2-phenylindole (DAPI) containing antifade solution (Vector Laboratories, Inc., Burlingame, CA). The nuclear morphology of cells was examined with a Leica DMRXA fluorescence microscope (Leica Mikroskopie and System, Wetzlar, Germany) equipped with appropriate epifluorescence filters and a COHU charge-coupled device camera. The rate of apoptosis was determined as the percentage of apoptotic nuclei of at least 500 nuclei/experimental group.

2.10. Cell cycle analysis

Adherent KB-3-1 cells (5×10^5 cells/well) were incubated in 6-well plates at 37 °C for 24 or 48 h with 0.5, 1, 2.5, 5 and 10 μM PF1022A. Cell cycle progression was analysed by flow cytometry using FACS Calibur (Becton Dickinson, Palo Alto, CA) as described [44]. Cell Quest Pro software (Becton Dickinson and Company, NY, USA) was used to analyse the resulting DNA histograms.

2.11. Detection of mitochondrial membrane potential

KB-3-1 cells (5×10^6 cells/well) were exposed to 1, 2.5, 5 and 10 μM PF1022A for 24 h before cell staining was performed with the fluorescent dye 5,5′,6,6′-tetrachloro-1,1′,3′,3′-tetraethyl-benzimidazolylcarbocyanine iodide (JC-1; Mitochondrial Membrane Potential detection Kit; Stratagene, La Jolla, CA, USA) as described [31,44].

2.12. Statistical analysis

Values are expressed as means ± S.E. where appropriate. Significance was calculated with Student's *t*-test for paired (f_c) and unpaired observations. Statistical significance was determined at levels of $P < 0.05$, $P < 0.01$ and $P < 0.001$.

3. Results

3.1. Effect on force of contraction

Isometrically measured f_c of isolated, pre-contracted (60 mM KCl) terminal ilea of the guinea pig was concentration-dependently (0.1–30 μM PF1022A) decreased with an IC_{50} of 25 ± 3 μM ($n = 3$). At solvent concentrations up to 3.5 μl methanol/Tween in 28 ml nutrient solution, which corresponds to the solvent concentration at 10 μM PF1022A, no effect on contractility of isolated smooth muscle preparations was observed. At 10 μl methanol/Tween in 28 ml nutrient solution, that is the solvent concentration at 30 μM PF1022A, f_c was decreased by 4.4% ($n = 3$). Therefore, results obtained with 30 μM PF1022A were corrected for this solvent induced decrease in contractility. Reduction of f_c was only significant at 30 μM PF1022A ($n = 3$, $P < 0.05$). At the anthelmintically active concentration of 1 μM PF1022A [6], the decrease of f_c from the control value of 17.8 ± 2.6 to 15.9 ± 2.2 mN was not significant ($n = 3$, $P > 0.05$).

3.2. Pore-forming activity

After a control period of 15 min during which no electrical activity could be observed at holding potentials between −60 and +60 mV, PF1022A was added to the bathing solution. 1–2 min after addition of 1 μM PF1022A pore-forming activity was detected in inside-out patches of Caco-2 cells with mono- and divalent cations (Na^+, K^+, Ca^{2+}) as the charge carriers. Higher PF1022A concentrations achieved similar effects, but faster onset of action and multiple channel openings (Fig. 1A). Washout of the substance was not effective indicating permanent incorporation into the cell membrane.

The experimental reversal potentials for potassium ($n = 3$) and sodium ($n = 3$) were comparable to the theoretical values for the ionic equilibrium potential calculated according to the Nernst equation. Further, current amplitudes did not vary when aspartate was substituted by chloride in the K^+ and Na^+ bathing solutions in equal cation molarity ($n = 3$), also indicating the channel's cationic selectivity.

Current to voltage relationships for potassium, sodium and calcium currents presented a symmetrical behaviour upon hyper- and depolarisation, rectifying at potentials higher than −20 and +20 mV. Single channel conductance was therefore estimated in the linear range of −20 to +20 mV and was calculated for K^+ at 39.3 ± 2.8 pS ($n = 5$), for Na^+ at 52.3 ± 3.0 pS ($n = 5$) and for Ca^{2+} at 50.5 ± 2.2 pS ($n = 3$).

Probability density functions for open times of the PF1022A channel conducting potassium, sodium or calcium ions at potentials ranging from −60 to +60 mV could be fitted with one exponential. The kinetics of the openings at those potentials was not significantly ($P > 0.05$) affected by voltage. Further, time constants for open times did not significantly differ for Na^+, K^+ and Ca^{2+} ($P > 0.05$). Open state probability was independent of voltage, however, varying markedly in different patches and also within one patch with time. Openings occurred usually in bursts of fast flickerings, which alternated with periods of electrical inactivity. For Ca^{2+} conducting channels these periods without electrical activity were almost twice the duration of those with the studied monovalent cations.

3.3. Effect on intracellular ion concentration

For studying the effect of PF1022A on intracellular calcium, sodium and potassium concentrations, the ionophores ionomycin, gramicidine and valinomycin ($n = 3$ for each) were used as reference compounds. Although PF1022A incorporated into the cell membrane leading to conduction of calcium, sodium and potassium ions, for Na^+ ions no effect on the intracellular concentration was observed, while the intracellular K^+ and Ca^{2+} concentrations were changed. The effect of PF1022A on intracellular Ca^{2+} concentration, however, was weak compared to the control with ionomycin. Representative recordings are presented for Ca^{2+} in Fig. 1B and C. Only a small increase in the intracellular Ca^{2+} concentration was caused by 100 μM PF1022A ($n = 7$) compared to 100 μM ionomycin, while at 10 μM PF1022A (a concentration causing multiple channel openings, see Fig. 1A, $n = 6$) no changes in $[Ca^{2+}]_i$ were observed (data not shown). The

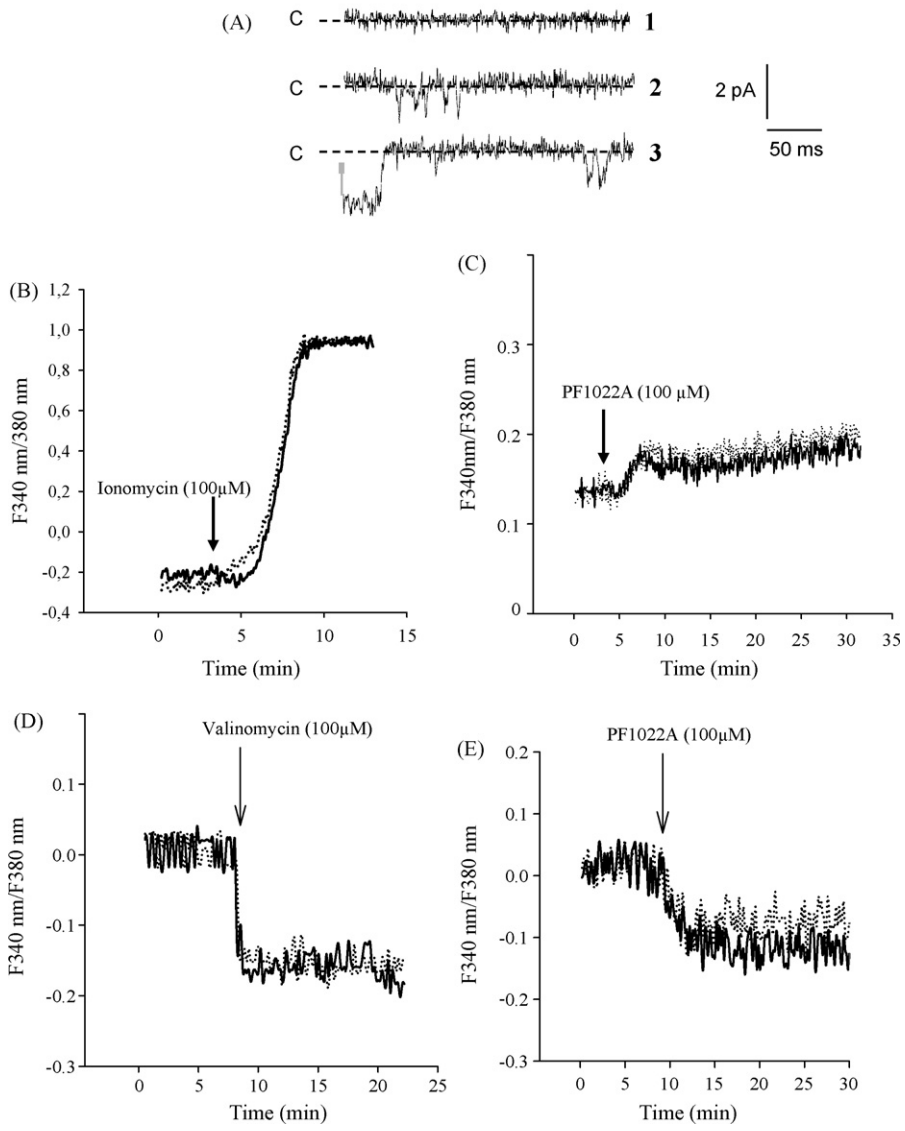

Fig. 1. Pore-forming activity and changes in intracellular ion concentrations. In (A) typical recordings of a Ca^{2+} current from an inside-out patch are shown. The dashed line marks the closed state "c"; downward deflections indicate channel openings. The holding potential was held at −60 mV. The upper trace 1 shows a control recording without openings. Traces 2 and 3 represent single and multiple channel openings in presence of 1 and 10 μM PF1022A, respectively. The small increase in intracellular Ca^{2+} concentration (expressed as ratio $F_{340\ nm}/F_{380\ nm}$) caused by 100 μM PF1022A (C) is shown for three representative cells in comparison to 100 μM ionomycin (B) (note the difference in scale on the ordinate). At 10 μM no changes in $[Ca^{2+}]_i$ were observed (data not shown). The effect on intracellular K^+ concentration is shown for 100 μM PF1022A (E) and 100 μM valinomycin (D) for two representative cells each.

effect on intracellular K^+ concentration is illustrated for 100 μM PF1022A (E) and 100 μM valinomycin (D) for two representative cells each. The effect on intracellular K^+ was more pronounced than on intracellular Ca^{2+}, but still weak at concentrations that already caused multiple channel openings (10 μM, $n = 6$), and ineffective at 1 μM PF1022A ($n = 5$).

3.4. Effect on chloride currents through $GABA_A$ channels by PF1022A

As an anthelmintic effect via binding to the GABA receptor in nematodes was suggested [27], we also studied the electrophysiological effect of PF1022A on $GABA_A$ channels. An effect on this channel is of interest e.g. in respect to sedative side effects of the drug. At 1 and 10 μM PF1022A, the potentiation of GABA-activated chloride current (I_{GABA}) through α1β2γ2S receptors was 20.8 ± 11.2% ($n = 4$) and 78.2 ± 16.1% ($n = 6$), respectively. However, an effect of PF1022A on $GABA_A$ can be excluded, because the solvent-induced increase in I_{GABA} was 70.8 ± 39.4% at a solvent concentration which corresponds to the concentration present at 10 μM PF1022A.

3.5. Effects of PF1022A on cell proliferation and viability

To investigate the impact of the anthelmintic drug PF1022A on human cell proliferation, dose-response curves (0.5–10 μM) were established in human KB-3-1 cells using different exposure times. Based on MTT assays an increased cell proliferation was observed in KB-3-1 cells after 24 and 48 h exposure to PF1022A concentrations ≤1 μM (Fig. 2). The maximal increase in cell growth (1.25-fold) was observed after 24 h incubation with 0.5 μM PF1022A. At higher PF1022A concentrations the number of viable cells decreased concentration dependently with an IC_{50} of 8.1 μM (24 h), 6.6 μM (48 h) and 5.9 μM (72 h), respectively.

Moreover, recovery of cells exposed for 1, 2, 4, 6, 8, 24 or 48 h to increasing PF1022A concentrations was studied after 72 h. These experiments revealed enhanced cell proliferation at concentra-

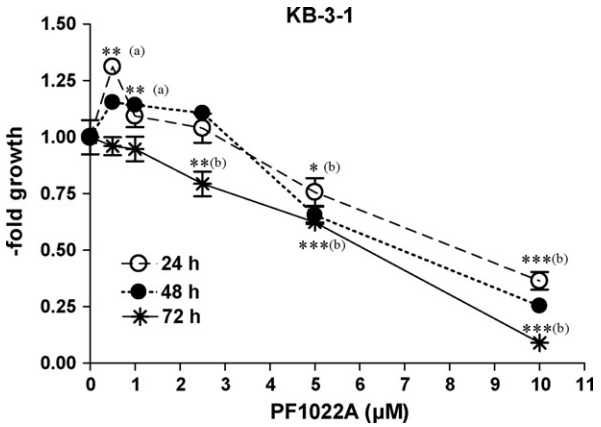

Fig. 2. Concentration-dependent effect on cell growth is demonstrated in KB-3-1 cells after exposure to PF1022A for 24, 48 and 72 h. After the respective treatment durations, drug solution was replaced by 100 μl MTT solution and viability was measured by a microplate reader, set at 450 nm with 620 nm as reference to reduce unspecific background values. All experiments were performed at least twice in triplicates. (a) Cell growth stimulating and (b) cytotoxic effects were significantly (*, **, ***: $P < 0.05$, <0.01, <0.001, respectively) different to untreated control (Student's *t*-test).

tions ≤2.5 μM and short exposure times (1–8 h). A maximum growth stimulation (1.3-fold growth) was obvious at 2 h treatment with 2.5 μM PF1022A. However, in experiments with expanded drug exposure time (24 and 48 h), no stimulating effect was observed (data not shown). This is in contrast to experiments without washout phase (Fig. 2). The cytotoxic effect at higher drug concentrations (>5 μM) and long time exposure (24 and 48 h) did not differ significantly from data obtained without washout. This indicates potent cytotoxic effects of PF1022A at high concentrations (data not shown).

3.6. Apoptosis induction by PF1022A

To gain more insights into the PF1022A-induced cell death, LDH release from mitochondria to cytosol, which is indicative for necrotic cell death, was measured. Since no cytosolic LDH was detectable after 24 h PF1022A treatment at concentrations ranging from 0.5 to 10 μM (data not shown), we hypothesized that the decrease in the number of viable cells was due to apoptotic cell death. This was further confirmed by results obtained by DAPI stainings of control and PF1022A-treated KB-3-1 cells. By direct counting under the microscope a concentration- and time-dependent increase of apoptotic nuclei was observed indicated by characteristic apoptotic features like cell shrinkage, chromatin condensation and apoptotic body formation. In more detail, after 24 h exposure to 2.5, 5 and 10 μM PF1022A a relative minor increase in the number of apoptotic nuclei from 2% in the control to 4%, 12% and 14% was observed (Fig. 3A). In contrast, after 48 h treatment with the above mentioned PF1022A concentrations the proportion of apoptotic nuclei remarkably increased from 3% in the control to 6%, 15% and 36%, respectively (Fig. 3B).

Since programmed cell death can be initiated via the so-called mitochondrial pathway which is based on depolarisation of the outer mitochondrial membrane, FACS analyses with JC-1-stained KB-3-1 cells were performed. JC-1 is a lipophilic cation fluorescent dye, which can enter into intact mitochondria selectively [44]. While after 24 h exposure to 10 μM PF1022A a moderate mitochondrial membrane depolarisation was shown (12.4% of cells vs. 4.3% in control) this effect was distinctly enhanced after 48 h treatment (32% of cells vs. control of 3%) (Fig. 4C). In contrast, PF1022A did not affect the mitochondrial membrane potential at concentrations ≤2.5 μM, independent of exposure time (data not shown).

3.7. Impact of PF1022A on cell cycle distribution

To further investigate whether PF1022A affect the cell cycle distribution flow cytometric analyses were performed in KB-3-1 cells and histograms were gated on live cells. PF1022A treatment caused a moderate concentration-dependent increase in the number of cells in G_0/G_1-phase after 24 and 48 h (Fig. 4). This effect was distinct at concentrations ≥5 μM as shown by an increase of cells in G_0/G_1-phase by 23% and 19% after 24 and 48 h exposure, respectively. Additionally, after 24 and 48 h treatment with 10 μM PF1022A a further increase was observed by 43% and 34%, respectively. In accordance, the number of cells in the S- and G_2/M-phase significantly decreased at these concentrations

3.8. Impact of apoptosis- and cell cycle-regulating proteins p53, p21, Bax, and Bcl-2 on PF1022A-induced cell death

To further investigate the mechanisms underlying PF1022A-induced cell death, the effect of apoptosis- and cell cycle-regulating proteins was studied. For this purpose, HCT116 cells with disrupted p53, p21 or bax genes as well as A549 cells with stably overexpressing bcl-2 gene (A549/Bcl-2) were used. In general, in all tested cell lines a distinct cytotoxic effect was observed at high concentrations (10 μM). Remarkably, deletion of p53 was accompanied with loss of sensitivity to high PF1022A concentrations (Table 1). Comparable effects were observed in HCT116 bax (−/−) cells (Table 1). In contrast, the cytotoxic effect of PF1022A was more prominent in HCT116 p21 (−/−) cells than in the respective parental cell clone (Table 1). Effects of PF1022A on cell growth of A549 with transfected Bcl2 and the A549 vector control did not differ significantly from each other.

4. Discussion

The anthelmintic drug PF1022A is active against diverse worms when administered orally or parenterally. Depending on the species of worms and the host, helmints are paralysed in concentrations ranging from 1 to 10 mg/kg body weight [8,26], which coincides with the *in vitro* activity at 1 μg/ml against *Trichinella spiralis* and *Nippostrongylus brasiliensis* [45] as well as the effect at 1 μM PF1022A against *H. contortus* [6]. The lack of an effect on f_c at 1 μM and an estimated IC_{50} of 25 μM for isolated guinea pig ileum demonstrate that contractility is not reduced significantly at anthelmintic active concentrations. Consequently, the peristalsis which is necessary to transfer food through the gut should not be affected by the drug. Comparable to other cyclohexadepsipeptides [46,47], PF1022A influenced the intracellular Ca^{2+} concentration in Caco-2 cells only at high drug concentrations (≥30 μM). Sustained Ca^{2+} elevation usually results in dysfunction of the contractile mechanism, which might be the cause of the observed reduction in the force of contraction in isolated guinea pig ileum at high drug concentrations.

Results obtained from electrophysiological experiments give evidence that the cyclooctadepsipeptide PF1022A interacts with mammalian cells. The drug was shown to incorporate into cell membranes forming cation selective channels, similar to the cyclohexadepsipeptides beauvericin [48] and enniatin [40]. Patch clamp studies revealed that PF1022A manifests common traits of physiological ion channel behaviour such as unitary transitions in conductance levels characteristic for channels, selectivity, rectification, and conductances in the pS range. This strongly suggests that PF1022A is a potential channel-forming ionophore. Moreover, formation of a sandwich complex can be postulated similar to the cyclohexadepsipeptides beauvericin [49] and enniatin [50]. Through such PF1022A-induced membrane spanning pores, ions are able to diffuse at both directions following their electrochemical gradient.

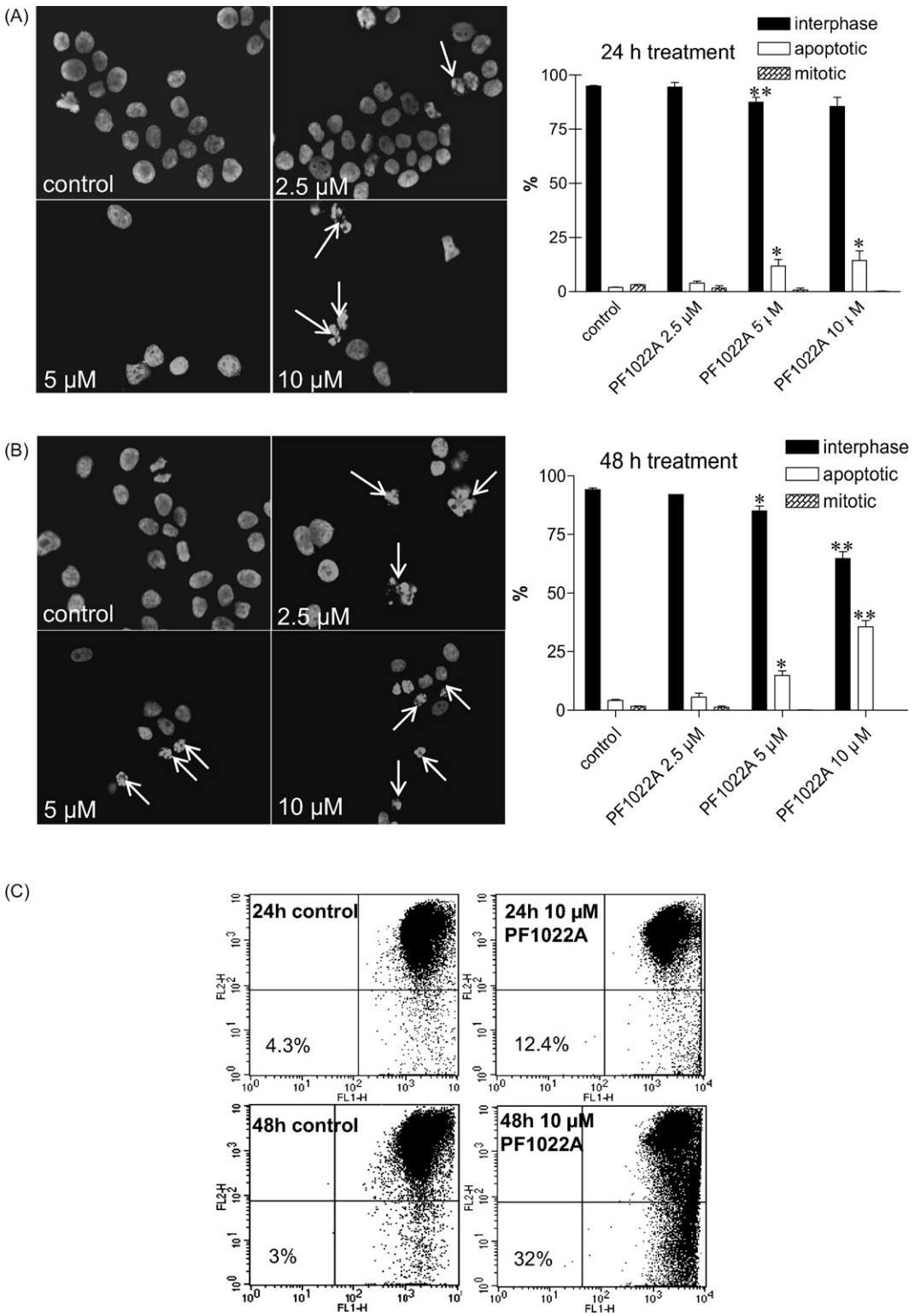

Fig. 3. (A and B) Nuclei of KB-3-1 cells were stained with DAPI, classified (in interphase, mitotic, and apoptotic) and counted. Means ± S.D. were calculated from at least 500 nuclei from three independent experiments. *, **, significant ($P < 0.05$, <0.01, respectively) difference between PF1022A-treated and -untreated cells was calculated using the Student's *t*-test. (C) Changes in the mitochondrial membrane potential were measured after 24 and 48 h of PF1022A treatment using the fluorescent dye JC-1. Percentages of apoptotic (green fluorescent, FL-1) cells, located in the right lower quarter, are indicated at the left bottom.

This conformation would allow the symmetry depicted in the current–voltage curves and the sort of electrostatic interaction that prevailed in our experiments, making the pore selective to cations. However, contrary to beauvericin and enniatin, the kinetics of the PF1022A-induced channel were not influenced by conducted cations. Although this ionophoric action was found already at very low drug concentrations, ion influx affected intracellular ion concentrations only minimally, even at high drug concentrations. Thus, these changes in intracellular ion concentrations might not contribute markedly to cellular toxicity. Apart from these findings, it

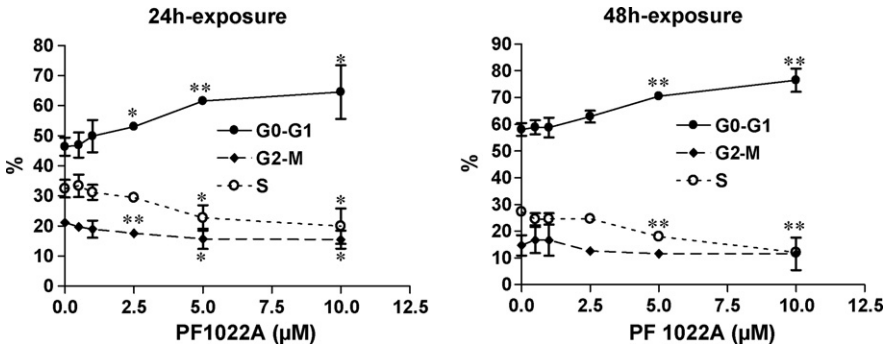

Fig. 4. PI staining and FACS analyses were performed on KB-3-1 cells after 24 and 48 h PF1022A exposure at the indicated drug concentrations. Percentages of cells in the G_0/G_1, S, and G_2/M phases of the cell cycle as well as apoptotic cells are indicated. *, **, significantly ($P < 0.05$, <0.01, respectively) different to untreated cells (Student's *t*-test).

has been already demonstrated that the ionophoric activity does not correlate with the anthelmintic potency of cyclooctadepsipeptides [28].

Besides the ionophoric activity, electrophysiological effects via modulation of the GABA current are discussed, as in binding studies it could be demonstrated that PF1022A binds to GABA receptors in nematodes, probably contributing to the anthelmintic effect [27]. Therefore, we tested whether PF1022A exerts any effect on $GABA_A$ receptors composed of α1, β2 and γ2S subunits, which might be of interest in terms of sedative side effects during anthelmintic therapy. Significant activation of the GABA current, however, was not observed.

For the reason of diverse pharmacological properties of structurally related compounds, and in order to prove low cellular toxicity of PF1022A at anthelmintic concentrations, a panel of cytotoxicity tests was performed in mammalian cells. Cytotoxic effects after different exposure times to PF1022A occurred at micromolar concentrations but higher than the active anthelmintic concentrations. Since the results obtained in experiments with and without washout phase did not differ significantly at PF1022A concentrations >5 μM and only a small number of cells could recover, a potent cytotoxic effect of this cyclooctadepsipeptide was suggested at high concentrations. In contrast, at low anthelmintic concentrations (0.5–1 μM) PF1022A significantly enhanced proliferation of the tumour cell line KB-3-1. Comparable effects were reported for the structurally related enniatins [31]. This growth stimulating activity was suggested to be based on compensatory mechanisms to enniatins-induced stress signals [31].

Regarding PF1022A-induced cytotoxicity, apoptosis induction via the mitochondrial pathway was suggested at least for long-term PF1022A treatment at high concentrations. This was based on a significant depolarisation of the mitochondrial membrane potential, which is an important step to trigger programmed cell death, after 48 h PF1022A treatment with 10 μM [50]. Moreover, several characteristics of programmed cell death like cell shrinkage, chromatin condensation and apoptotic body formations were observed after 48 h drug treatment with 10 μM PF1022A. Furthermore, the complete lack of cellular lactate dehydrogenase release indicative for necrotic cell death emphasizes the apoptotic activity of the anthelmintic drug. These results are comparable to the cytototoxic effects of the structurally related cyclohexadepsipeptides enniatins [31] and beauvericin [32,33]. Moreover, since the ionophoric activity of these cyclic peptides was suggested to contribute to their potent cytotoxicity [33,46,51], comparable modes of actions might be hypothesized for PF1022A. However, our study revealed that only high concentrations (100 μM) of the cyclooctadepsipeptide PF1022A cause an increase in the intracellular Ca^{2+} levels. Thus, this effect does not seem to contribute markedly to cytotoxicity.

In addition to apoptosis induction, our study revealed that long-term but also short-term PF1022A treatment concentration-dependently led to cell cycle arrest in G_0/G_1 phase. Thus, the cytotoxic modes of actions of short-term PF1022A exposure might be based on a cell cycle blockade. Consistently, data obtained by DAPI staining revealed a significant reduction of countable nuclei compared to control after 24 h drug treatment. Moreover, cells with deleted cyclin-dependent kinase inhibitor p21 were more sensitive to PF1022A-induced cytotoxicity. This suggests that cell cycle blockade via p21 might rescue cells from PF1022A-induced cell death as it was also suggested for the structurally related enniatins [31].

To further investigate the impact of PF1022A on apoptosis- and cell cycle-regulating proteins, HCT116 cells with disrupted p53, p21 or bax genes [37–39] and A549 cells transfected with Bcl-2 were used. In MTT assays, a small shift of cytotoxicity to higher PF1022A concentrations was observed in p53 and bax disrupted cells, whereas the apoptosis inhibitor Bcl-2 had no significant influence on PF1022A-induced cell death. Thus, our data suggest that PF1022A-induced mitochondrial membrane depolarisation occurs via a molecular mechanism involving p53-mediated apoptosis effects. This is in contrast to enniatins, which mediated apoptosis induction independent of either of these proteins, but activated the proapototic p53-downstream target bax at relatively low enniatin concentrations [31].

To conclude, data obtained with PF1022A in mammalian tissue and cells point to drug safety in terms of lower susceptibility of mammalian tissue compared to the paralysing effect in helmints. Moreover, due to the lack of an effect on $I_{GABA(A)}$ at anthelmintic concentrations no sedative side effects are to be expected. In addition, the drug PF1022A and its derivatives might be of interest to be studied in more detail in respect to anticancer activity.

Table 1
Impact of apoptosis- and cell cycle-regulating proteins p53, p21, Bax, and Bcl-2 on PF1022A-induced cell death. IC_{50} values (μM) for the time-dependent cytotoxic effect of PF1022A are given.

Cell line	48 h	72 h
HCT 116 p53 (+/+)	8.4 ± 0.1	7.5 ± 0.1
HCT 116 p53 (−/−)	9.6 ± 0.3	9.1 ± 0.1
HCT 116 bax (+/+)	7.4 ± 0.3	7.1 ± 0.1
HCT 116 bax (−/−)	9.5 ± 0.1	8.2 ± 0.1
HCT 116 p21 (+/+)	9.4 ± 0.1	8.2 ± 0.1
HCT 116 p21 (−/−)	6.0 ± 0.1	4.6 ± 0.1
A549/Bcl-2	7.5 ± 0.1	4.3 ± 0.2
A549/vc	7.3 ± 0.1	4.6 ± 0.1

References

[1] Bundy DA, de Silva NR. Can we deworm this wormy world? Br Med Bull 1998;54:421–32.

[2] Waller PJ. Anthelmintic resistance. Vet Parasitol 1997;72:391–412.
[3] von Samson-Himmelstjerna G, Harder A, Sangster NC, Coles GC. Efficacy or two cyclooctadepsipeptides, PF1022A and emodepsidde, against anthelmintic-resistant nematodes in sheep and cattle. Parasitology 2005;130:343–7.
[4] Geary TG, Sangster NC, Thompson DP. Frontiers in anthelmintic pharmacology. Vet Parasitol 1999;84:275–95.
[5] Sasaki T, Takagi M, Yaguchi T, Miyadoh S, Okada T, Koyama M. A new anthelmintic cyclodepsipeptide, PF1022A. J Antibiot (Tokyo) 1992;45:692–7.
[6] Conder GA, Johnson SS, Nowakovski DS, Blake TE, Dutton FE, Nelson SJ, et al. Anthelmintic profile of the cyclodepsipeptide PF1022A in in vitro and in vivo models. J Antibiot (Tokyo) 1995;48:820–3.
[7] Kachi S, Terada M, Hashimoto H. Effect of PF1022A on adult *Angiostrongylus cantonensisin* the pulmonary arteries and larvae migrating into the central nervous system in rats. Parasitol Res 1995;81:631–7.
[8] von Samson-Himmelstjerna G, Harder A, Schmieder T, Kalbe J, Mencke N. In vivo activities of the new anthelmintic depsipeptide PF1022A. Parasitol Res 2000;86:194–9.
[9] Zahner H, Taubert A, Harder A, von Samson-Himmelstjerna G. Filaricidal efficacy of anthelmintically active cyclodepsipeptides. Int J Parasitol 2001; 31:1515–22.
[10] Mentz MB, Graeff-Teixeira C. Drug trials for treatment of human angiostrongliasis. Rev Inst Med Trop Sao Paulo 2003;45:179–84.
[11] Weckwerth W, Miyamoto K, Iinuma K, Krause M, Glinski M, Storm T, et al. Biosynthesis of PF1022A and related cyclooctadepsipeptides. J Biol Chem 2000;275:17909–15.
[12] Krause M. Untersuchungen zur Biosynthese des Cyclooctadepsipeptids PF1022A. Dissertation, TU, Berlin; 1998.
[13] Yanai K, Sumida N, Okakura K, Moriya T, Watanabe M, Murakami T. Para-position derivatives of fungal anthelmintic cyclodepsipeptides engineered with *Streptomyces venezuelae* antibiotic biosynthetic genes. Nat Biotechnol 2004;22:848–55.
[14] Jeschke P, Iinuma K, Harder A, Schindler M, Murakami T. Influence of the cyclooctadepsipeptide PF1022A and PF1022E as natural products on the design of the semi-synthetic anthelmintics such as emodepside. Parasitol Res 2005;97:511–6.
[15] Jeschke P, Harder A, Etzel W, Gau W, Thielking G, Bonse G, et al. Synthesis and anthelmintic activity of thioamide analogues of cyclic octadepsipeptides such as PF1022A. Pest Manage Sci 2001;57:1000–6.
[16] Jeschke P, Harder A, von Samson-Himmelstjerna G, Etzel W, Gau W, Thielking G, et al. Synthesis of anthelmintically active N-methylated amidoxime analogues of the cyclic octadepsipeptide PF1022A. Pest Manage Sci 2002;58:1205–15.
[17] Dyker H, Harder A, Scherkenbeck J. Chimeric cyclodepsipeptides as mimetics for the anthelmintic PF1022A. Bioorg Med Chem Lett 2004;14:6129–32.
[18] Dutton FE, Nelson SJ. Synthesis of PF1022A, an anthelmintic cyclodepsipeptide. J Antibiot (Tokyo) 1994;47:1322–7.
[19] Dutton FE, Lee BH, Johnson SS, Coscarelli EM, Lee PH. Restricted conformation analogues of an anthelmintic cyclodepsipeptide. J Med Chem 2003;46:2057–73.
[20] Lee BH, Dutton FE, Thompson DP, Thomas EM. Generation of a small library of cyclodepsipeptide PF1022A analogues using a cyclization-cleavage method with oxime resin. Bioorg Med Chem Lett 2002;12:353–6.
[21] Scherkenbeck J, Jeschke P, Harder A. PF1022A and related cyclodepsipeptides—a novel class of anthelmintics. Curr Top Med Chem 2002;2:759–77.
[22] Scherkenbeck J, Harder A, Plant A, Dyker H. PF1022A—a novel anthelmintic cyclooctadepsipeptide. Modification and exchange of the N-methyl leucine residues. Bioorg Med Chem Lett 1998;8:1035–40.
[23] Saeger B, Schmitt-Wrede HP, Dehnhardt M, Benten WPM, Krücken J, Harder A, et al. Latrophilin-like receptor from the parasitic nematode *Haemonchus contortus* as target for the anthelmintic depsipeptide PF1022A. FASEB J 2001;15:1332–54.
[24] Harder A, Schmitt-Wrede, Krücken J, Marinovski P, Wunderlich F, Willson J, et al. Cyclooctadepsipeptides—an anthelmintically active class of compounds exhibiting a novel mode of action. Int J Antimicrob Agents 2003;22:318–31.
[25] Harder A, Holden-Dye L, Walker R, Wunderlich F. Mechanisms of action of emodepside. Parasitol Res 2005;97:S1–0.
[26] Harder A, von Samson-Himmelstjerna G. Cyclooctadepsipeptides—a new class of anthelmintically active compounds. Parasitol Res 2002;88:481–8.
[27] Chen W, Terada M, Cheng JT. Characterization of subtypes of gamma-aminobutyric acid receptors in an *Ascaris* muscle preparation by binding assay and binding of PF1022A, a new anthelmintic, on the receptor. Parasitol Res 1996;82:97–101.
[28] Gessner G, Meder S, Rink T, Boheim G, Harder A, Jeschke P, et al. Ionophore and anthelmintic activity of PF1022A, a cyclooctadepsipeptide, are not related. Pest Sci 1996;48:399–407.
[29] Zhang L, Yan K, Zhang Y, Huang R, Bian J, Zheng C, et al. High-throughput synergy screening identifies microbial metabolites as combination agents for the treatment of fungal infections. Proc Natl Acad Sci USA 2007;104:4606–11.
[30] Fukuda T, Arai M, Yamaguchi Y, Masuma R, Tomoda H, Omura S. New beauvericins, potentiators of antifungal miconazole activity, produced by *Beauveria* sp. FKI-1366. Taxonomy, fermentation, isolation and biological properties. J Antibiot 2004;57:110–6.
[31] Dornetshuber R, Heffeter P, Kamyar M, Peterbauer T, Berger W, Lemmens-Gruber R. Enniatin induces apoptosis and exerts p53-dependent cytostatic and p53-independent cytotoxic activities against human cancer cells. Chem Res Toxicol 2007;20:465–73.
[32] Lin HI, Lee YJ, Chen BF, Tsai MC, Lu JL, Chou CJ, et al. Involvement of Bcl-family, cytochrome c and caspase 3 in induction of apoptosis by beauvericin in human non-small cell lung cancer cells. Cancer Lett 2005;239:248–59.
[33] Jow GM, Chou CJ, Chen BF, Tsai JH. Beauvericin induces cytotoxic effects in human acute lymphoblastic leukemia cells through cytochrome c release, caspase 3 activation: the causative role of calcium. Cancer Lett 2004;216: 165–73.
[34] Zhan J, Burns AM, Liu MX, Faeth SH, Gunatilaka AAL. Search for cell motility and angiogenesis inhibitors with potential anticancer activity: beauvericin and other constituents of two endophytic strains of *Fusarium oxysporum*. J Nat Prod 2007;70:227–32.
[35] Jeschke P, Benet-Buchholz J, Harder A, Etzel W, Schindler M, Gau W, et al. Synthesis and anthelmintic activity of substituted (R)-phenyllactic acid containing cyclohexadepsipeptides. Bioorg Med Chem Lett 2006;16:4410–5.
[36] Shen DW, Cardarelli C, Hwang J, Cornwell M, Richert N, Ishii S, et al. Multiple drug-resistant human KB carcinoma cells independently selected for high-level resistance to colchicine, adriamycin, or vinblastine show changes in expression of specific proteins. J Biol Chem 1986;261:7762–70.
[37] Bunz F, Fauth C, Speicher MR, Dutriaux A, Sedivy JM, Kinzler KW, et al. Targeted inactivation of p53 in human cells does not result in aneuploidy. Cancer Res 2002;62:1129–33.
[38] Waldman T, Kinzler KW, Vogelstein B. p21 is necessary for the p53-mediated G1 arrest in human cancer cells. Cancer Res 1995;55:5187–90.
[39] Zhang L, Yu J, Park BH, Kinzler KW, Vogelstein B. Role of BAX in the apoptotic response to anticancer agents. Science 2000;290:989–92.
[40] Kamyar MR, Rawnduzi P, Studenik C, Kouri K, Lemmens-Gruber R. Investigation of the electrophysiological properties of enniatin. Arch Biochem Biophys 2004;429:215–23.
[41] Khom S, Baburin I, Timin EN, Hohaus A, Sieghart W, Hering S. Pharmacological properties of $GABA_A$ receptors containing gamma1 subunits. Mol Pharmacol 2006;69:640–9.
[42] Methfessel C, Witzemann V, Takahashi T, Mishina M, Numa S, Sakmann B. Patch clamp measurements on *Xenopus laevis* oocytes: currents through endogenous channels and implanted acetylcholine receptor and sodium channels. Pflugers Arch 1986;407:577–88.
[43] Baburin I, Beyl S, Hering S. Automated fast perfusion of *Xenopus* oocytes for drug screening. Pflugers Arch 2006;453:117–23.
[44] Heffeter P, Jakupec MA, Körner W, Chiba P, Pirker C, Dornetshuber R, et al. Multidrug-resistant cancder cells are preferential targets of the new antineoplastic lanthanum compound KP772 (FFC24). Biochem Pharmacol 2007;73: 1873–86.
[45] Martin RJ, Harder A, Londerhausen M, Jeschke P. Anthelmintic actions of the cyclic depsipeptide PF1022A and its electrophysiological effects on muscle cells of *Ascaris suum*. Pest Sci 1996;48:343–9.
[46] Kouri K, Duchen MR, Lemmens-Gruber R. Effects of beauvericin on the metabolic state and ionic homeostasis of ventricular myocytes of the guinea pig. Chem Res Toxicol 2005;18:1661–8.
[47] Kamyar MR, Kouri K, Rawnduzi P, Studenik C, Lemmens-Gruber R. Effects of moniliformin in presence of cyclohexadepsipeptides on isolated mammalian tissue and cells. Toxicol In Vitro 2006;20:1284–91.
[48] Kouri K, Lemmens M, Lemmens-Gruber R. Beauvericin induced channels in ventricular myocytes and artificial membranes. Biochim Biophys Acta 2003; 1609:203–10.
[49] Ivanov VT, Evstratov AV, Sumskaya LV, Melnik EI, Chumburidze TS, Portnova SL, et al. Sandwich complexes as a functional form of the enniatin ionophores. FEBS Lett 1973;36:65–71.
[50] Ovchinnikov YA, Ivanov VT, Evstratov AV, Mikhaleva II, Bystrov VF, Portnova SL, et al. The enniatin ionophores. Conformation and ion binding properties. Int J Peptide Protein Res 1974;6:465–98.
[51] Tang Y, Chen YW, Jow GM, Chou CJ, Jeng CJ. Beauvericin activates Ca^{2+}-activated Cl^- currents and induces cell deaths in *Xenopus* oocytes via influx of extracellular Ca^{2+}. Chem Res Toxicol 2005;18:825–33.